

Electronic properties of quantum-dot superlattices

J. A. Brum*

Walter Schottky Institut, Technische Universität München, Am Coulombwall D-8046 Garching, Federal Republic of Germany
(Received 27 November 1990)

The electronic properties of a corrugated one-dimensional (1D) channel, forming an open-quantum-dot superlattice, are studied. The miniband dispersion is calculated and the transmission probability through the channel is analyzed as a function of the number of dots. Two further features are predicted in addition to the existence of superlattice gaps originating from the periodicity: the tunneling through the quantum-dot state before the first 1D channel is available for transmission and the quantum-dot gaps.

Since the paper of Esaki and Tsu,¹ an enormous amount of work has been produced in fundamental physics as well as in the applications^{2,3} of the two-dimensional (2D) electron gas and analog systems. With the improvement of the lithographic techniques, it has become possible to confine the carriers in additional directions and thus create quasi-one-dimensional (1D) and quasi-0D electron gases. Ballistic transport in high-mobility structures has shown nice effects due to the 1D quantization in narrow channels.⁴ A natural extension is the construction of dots (or open dots), which have been studied both experimentally⁵ and theoretically.⁶ Recently, the effect of the coupling among opened quantum dots has also been experimentally investigated.^{7,8}

In this communication we investigate a superlattice consisting of an array of quantum dots connected by one-dimensional channels. We consider a structure with strong confinement along the z direction (the epitaxial-growth direction) so that the system is in the electric quantum limit with respect to quantization of motion in this direction. The lateral confinement shows a periodic variation on its width as shown in Fig. 1. The main difference to the previous man-made superlattices is the

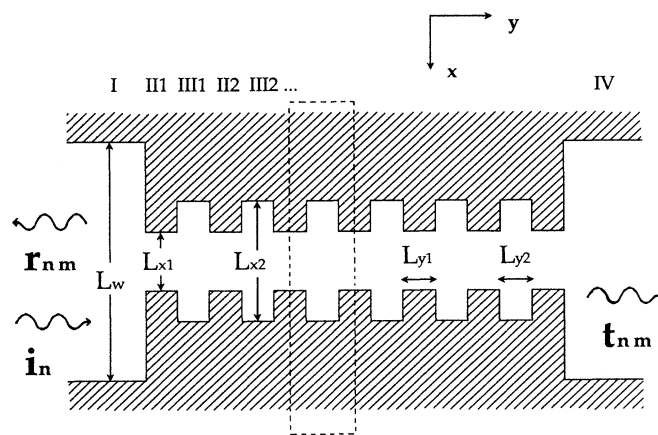


FIG. 1. A schematic illustration of the confining potential used in the calculations.

dimensionality of the continuum and of the states forming the superlattice. Here, we have 0D states embedded inside the 1D channel formed by the lateral confinement. First, we calculate the miniband dispersion for the open-quantum-dot (OQD) superlattice. The transmission coefficient is then obtained for a finite number of quantum dots. The features observed are well understood by mapping the miniband dispersion into the transmission channels. For high-purity samples, it is possible to obtain ballistic transport through a large extension, enough to include several dots.^{7,8} In this case, the quantum features will be reflected in the transport measurements. Our results give additional qualitative insight to the recent experimental findings in the ballistic transport measurements through a finite number of OQD's.^{7,8} Ulloa, Castaño, and Kirczenow⁹ calculated the conductance for a five-OQD structure. They associated the antiresonances in the conductance with gaps originated from the periodicity of the dots. Here, we demonstrate the existence of two different kinds of transmission gaps and explain their origin.

We focus on the conduction band and consider a typical finite-square-well confinement in the z and x motions for each region of the structure sketched in Fig. 1. We use the envelope function approximation³ and consider the z motion decoupled from the (x,y) motion.¹⁰ The zero of energy is chosen at the edge of the ground z -related subband and we neglect any further effect from the z confinement. To find the solutions we use the basis of solutions obtained for the x -confinement well of the larger regions (I and IV) [$a_m(x)$'s and respective eigenvalues ϵ_m 's]. The solutions for the other regions (III, IIII, etc.) are searched by projecting the Hamiltonian onto this basis and they are written

$$f_{Wl}(x,y) = \sum_{j=1}^M (d_j^{Wl} e^{ik_j y} + e_j^{Wl} e^{-ik_j y}) \sum_{n=1}^M a_n^{Wl}(k_j^2) a_n(x), \quad (1)$$

where M is the number of states considered in the basis, $W=II,III$, and $l=1,2,\dots,N$, with N being the number of periods. k_j 's are the eigenvalues and $a_n^{Wl}(k_j)$'s the eigenvectors for a fixed energy ϵ of the incident wave and

for a given channel, obtained by solving the system

$$\left(\frac{\hbar^2 k_j^2}{2m^*} + \varepsilon_n - \varepsilon \right) a_n^{WI} + V_b \sum_{m=1}^M a_m^{WI} \langle \alpha_n | Y(L_w^2/4 - x^2) - Y(L_{x\omega}^2/4 - x^2) | \alpha_m \rangle = 0, \quad n=1,2,3,\dots,M \quad (2)$$

for the symmetric structure. Here, $Y(x)$ is the unit-step function [$Y(x)=1$ if $x > 0$ and 0 otherwise], V_b is the barrier height, and $\omega=1,2$. k_j may assume complex values in order to include the evanescent part of the wave function in the barriers. With this approach, we may modify the shape of the lateral confinement without the necessity to generate a new basis at each step. We include as many eigenfunctions in our basis as it is necessary to obtain a desired convergence in the solutions. We find the miniband dispersion by using the boundary conditions inside the unit cell (dashed line in Fig. 1) plus the Bloch condition.

In Fig. 2 we plot the miniband dispersion for two cases: (a) an x -symmetric OQD superlattice and (b) an asymmetric one, where one of the sides of the 1D channel is flat. As a consequence of the perfect symmetry, the minibands in Fig. 2(a), originating from the even and odd- x -related subbands, do not interact. They form two independent sets with the same qualitative behavior. We concentrate our analysis on the even- x minibands [solid

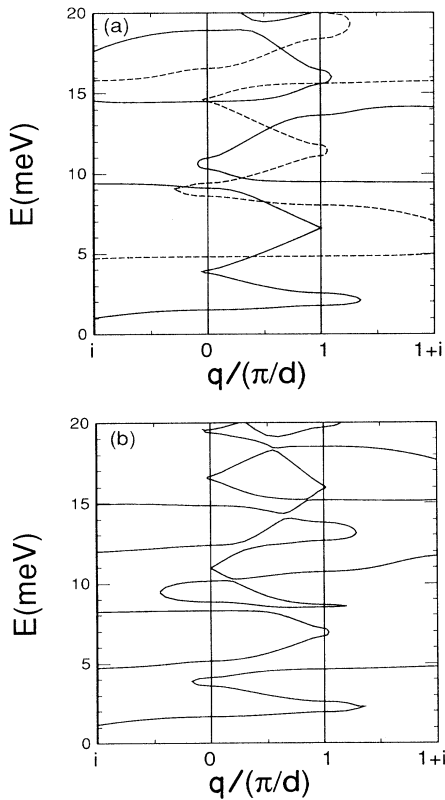


FIG. 2. Miniband dispersion for a quantum-dot superlattice with (a) symmetric dots and (b) the dots in only one of the sides. $V_b=600$ meV, $L_{x1}=500$ Å, $L_{x2}=800$ Å, $L_{y1}=L_{y2}=500$ Å, $d=L_{y1}+L_{y2}$.

line in Fig. 2(a)]. Basically, we observe the formation of minibands by folding the Brillouin zone, creating direct gaps. The first miniband, in particular, originates from the coupling between the localized states of the OQD. These states are confined by the lateral barriers and the 1D quantization in the channel, forming a small barrier through which they can tunnel. In addition to these minibands, there is the interaction between the 1D miniband (without constriction) and the virtual-OQD states, creating anticrossing between those states at the virtual-OQD states energy and, consequently, indirect gaps. At higher energies, when the second 1D channel state is reached, the interaction between the paths and the virtual-OQD states generates a quite complex miniband structure with some miniband minima outside the symmetry points. A similar dispersion is observed for the minibands originated from the odd- x -related levels (dashed lines). For the asymmetric superlattice, the even and odd modes interact among themselves and additional anticrossings are observed.

To probe the electronic properties of the OQD superlattice, we calculate the transmission coefficients through a finite number of dots. We “close” the OQD superlattice by two additional interfaces, linking the two wide regions of Fig. 1. We calculate the wave functions per layer following the procedure described by Eqs. (1) and (2). The coefficients are determined by matching the wave functions and the fluxes at the interfaces. This leads us to a $4(N+1)M$ nonhomogeneous linear system of equations which is calculated numerically for a particular incident mode.¹⁰ In Fig. 3 we plot the total transmission coefficient, $T = \sum_{m,n} (q_m/q_n) |t_{nm}|^2$ (here, q_n is the wave vector of the incoming mode, q_m is the wave vector of the out-

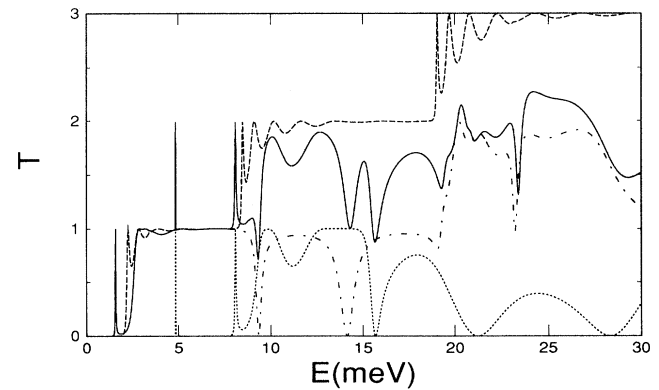


FIG. 3. Total transmission coefficient as a function of the incident energy for (a) a single-symmetric OQD (solid line) and a single constriction ($L=2L_{y1}+L_{y2}$) (dashed line). The separate contributions of the even (dash-dotted line) and the odd (dotted line) modes are also shown. $L_w=2000$ Å; the other parameters are the same as in Fig. 2.

going mode, and t_{nm} is the coefficient of the m th outgoing mode for the n th incoming mode,¹⁰ and the sum is over the propagative modes), as a function of the energy of the incident electron for a symmetric single-OQD structure (solid line) and the independent contributions of the even (dashed line) and odd modes (dash-dotted line). The flat channel—single constriction—is also shown. This is identical to the result obtained by other authors⁴ to interpret the step quantization of the conductance observed by van Wees *et al.*¹¹ and Wharam *et al.*¹² The main qualitative features in the transmission coefficient can be analyzed by considering the transfer matrix approach. In this case, if we call \mathbf{R} and \mathbf{T} the vectors defining the wave functions in the left-wide and right-wide regions, respectively, we can write

$$\mathbf{T} = \underline{S}_2 \underline{T}^N \underline{S}_1^{-1} \mathbf{R} = \underline{S}_2 \underline{U} \underline{\Gamma}^N \underline{U}^{-1} \underline{S}_1^{-1} \mathbf{R}. \quad (3)$$

Here, \underline{T} is the transfer matrix, $\underline{\Gamma}$ is a diagonal matrix formed by the eigenvalues of the transfer matrix, λ 's, and \underline{U} 's are the unitary matrix of the transformation. \underline{S}_1 and \underline{S}_2 are the matrixes relating the left-wide region and the right-wide region to the more constricted one. The transfer matrix eigenvalues λ 's can be mapped from the miniband dispersion by the relation $\lambda = e^{iqd}$. Transmission is only possible through the open channels, when $|\lambda| = 1$. For $|\lambda| \neq 1$, the electron wave function decays from one site of the superlattice to the next. Now we explain the two different kinds of transmission gaps: (a) the superlattice gaps, associated with the periodicity of the structure, and (b) the quantum-dot gaps, associated with the dimensionality of the structure. The quantum-dot gaps are indirect gaps in the dispersion relation resulting from the anticrossing between a virtual-OQD level and a precise k_y 1D state. A single dot is therefore enough to open a transmission gap since the $\text{Im}(q)$ values are too large in the indirect gaps to allow any transmission. The superlattice gaps are the direct gaps in the dispersion relation. For energies in these gaps, $|\lambda| \sim 1$, the decaying of the electron wave function is slow. For a finite structure with few dots, transmission is still possible. Effectively, by comparing Fig. 2(a) and Fig. 3, for the single-OQD structure, we observe that the transmission gaps are dominated by the quantum-dot gaps. The only superlattice gap present is associated with the gap between the 0D cavity-bound state and the 1D continuum ($1.94 \text{ meV} < \varepsilon < 2.59 \text{ meV}$)—the conductance threshold for the single-constriction case. This sharp resonance from the 0D-1D-0D tunneling allows transmission before the first 1D channel is open for transmission and originates the first miniband in the multidot structure (Fig. 4). When the number of dots increases, superlattice transmission gaps open as a consequence of the relation $\lambda^N = e^{iNqd}$ in Eq. (3), since for those energies the q 's are all imaginary and the incoming wave decays more rapidly with N . Most of the superlattice gaps are already transmission gaps for the 10-OQD structure. For a structure showing a large number of dots, the different origins of the gaps are indistinguishable from the transmission point of view.

When the second 1D path is energetically available, the transmission increases and reaches a value close to 2, reflecting the existence of two branches in the energy

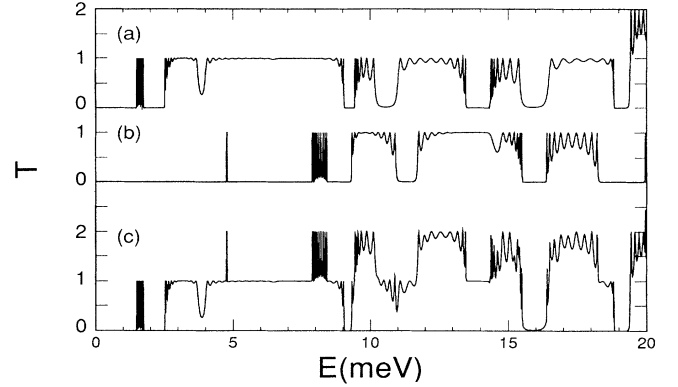


FIG. 4. Total transmission coefficient as a function of the incident energy for the 10-symmetric-OQD structure for the (a) even modes, (b) odd modes, and (c) the contributions of both even and odd modes. The parameters are the same as in Fig. 3.

dispersion in $\text{Re}(q)$. Now the anticrossing between the 0D and 1D states eliminates only one of the paths keeping the other path open, and the transmission falls to 1 instead of 0. Once the gaps in transmission are well defined in the multi-OQD, we observe between them a number of oscillations equal to the number of dots. They are related to the Bloch-type states, in a tight-binding band, formed by the overlap of the quasibound states in the constrictions of the superlattice. Whenever the gaps from the even and odd mode overlap, the transmission coefficient drops from a value close to 2 to 0. For the asymmetric case, the transmission coefficient changes according to the miniband dispersion shown in Fig. 2(b). New gaps open due to the anticrossing between the even and odd minibands. However, the analysis of the total symmetric OQD structure still helps to understand the main features in the transmission coefficient in terms of the miniband dispersion.

So far, we have considered the case of sharp interfaces. This approximation might introduce effects due to the reflections of the interfaces, creating Fabry-Pérot-type oscillations in the transmission coefficients. These effects are difficult to observe experimentally in actual samples because of the smoothness of the self-consistent potential.¹³ The sharp interfaces in our model introduce scattering of the incident waves into different subbands.¹⁰ We can approach the quasiadiabatic case and destroy the Fabry-Pérot structures by smoothing the sharp interfaces. This is achieved by replacing each modulated region (II,III's) by a series of regions with a fixed step in the y direction, following a Gaussian shape once the step goes to zero. Although we do not obtain full adiabaticity, the Fabry-Pérot oscillations for a 1500-Å single constriction disappear completely. In the case of the quantum dot, when the previous four interfaces of the sharp structure are replaced by 20 interfaces, separated by 100 Å in y , there is no qualitative change in the transmission. This demonstrates the observed structures are associated with the miniband dispersion.

A direct comparison between our results and the experimental results is somewhat difficult. The potential profile

of the actual structures is determined by the self-consistent charge transfer. The conductance measurements are obtained by varying the applied gate voltage that defines the structure. Both the Fermi energy and the geometric structure change. In addition, for real structures the relation between the gate voltage and the geometry is not well defined. Also, because the structure is small, charging effects,¹⁴ which are present in transport measurements, might have the same scale in energy as the miniband dispersion. Recently, Kouwenhoven *et al.*⁷ observed very clear gaps in the conductance as a function of the gate voltage for a 15-asymmetric-dot structure in the presence of a magnetic field to enhance the adiabaticity. They also observe the oscillations between the gaps, asso-

ciated with the finite number of dots in the structure, as confirmed here. Haug *et al.*⁸ have observed similar results for three- and four-dot structures.

The author would like to thank G. Bastard, C. Gonçalves da Silva, W. Hansen, J. M. Hong, P. Schulz, and D. Wharam for valuable discussions and P. Vogl for suggestions on the manuscript. The author would also like to thank the Laboratório Nacional de Luz Síncrotron (Brazil) for the numerical facilities kindly made available for the portion of the work developed in Brazil. The author would like to thank the Alexander von Humboldt Foundation for financial support.

*Permanent address: Instituto de Física, University of Campinas, 13081-Campinas, São Paulo, Brazil.

¹L. Esaki and R. Tsu, IBM J. Res. Dev. Lab., Portland Cem. Assoc. **14**, 61 (1970).

²*Heterojunction Band Discontinuities: Physics and Device Applications*, edited by F. Capasso and G. Magaritondo (North-Holland, Amsterdam, 1987), and references cited therein.

³G. Bastard, *Wave Mechanics Applied to Semiconductor Heterostructures* (Les Editions de Physique, Les Ulis, 1988).

⁴C. W. J. Beenakker and H. van Houten, *Solid State Physics*, edited by H. Ehrenreich and D. Turnbull (Academic, New York, in press), and references cited therein.

⁵B. J. van Wees, L. P. Kouwenhoven, C. J. P. M. Harmans, J. G. Williamson, C. E. Timmering, M. E. I. Broekaart, C. T. Foxon, and J. J. Harris, Phys. Rev. Lett. **62**, 2523 (1989); C. G. Smith, M. Pepper, H. Ahmed, J. E. F. Frost, D. G. Hasko, D. C. Peacock, D. A. Ritchie, and G. A. Jones, J. Phys. C **21**, L893 (1988); Y. Hirayama and T. Saku, Phys. Rev. B **41**, 2927 (1990).

⁶D. van der Marel, in *Nanostructures Physics and Fabrication — 1989, College Station, Texas*, Proceedings of the International Symposium, edited by M. A. Reed and W. P. Kirk (Academic, New York, 1990), p. 149; C. Lent, S. Sivaprasam, and D. J. Kirkner, *ibid.*, p. 279; F. M. Peeters, *Science and Engineering of 1- and 0-Dimensional Semiconductors*, NATO ASI Series, edited by S. P. Beaumont and C. M. So-

tomayor Torres (Plenum, New York, 1990), p. 107.

⁷L. P. Kouwenhoven, F. W. J. Hekking, B. J. van Wees, C. J. P. M. Harmans, C. E. Timmering, and C. T. Foxon, Phys. Rev. Lett. **65**, 361 (1990); L. P. Kouwenhoven, B. J. van Wees, B. van der Enden, and K. J. P. M. Harmans, in *Proceedings of the 20th International Conference on Physics of Semiconductors*, edited by J. Joannopoulos (World Scientific, London, 1990), p. 2325.

⁸R. J. Haug, K. Y. Lee, T. P. Smith III, and J. M. Hong, in *Proceedings of the 20th International Conference on Physics of Semiconductors*, edited by J. Joannopoulos (World Scientific, London, 1990), p. 2443.

⁹S. E. Ulloa, E. Castaño, and G. Kirczenow, Phys. Rev. B **41**, 12350 (1990).

¹⁰J. A. Brum and G. Bastard, in *Science and Engineering of 1- and 0-Dimensional Semiconductors*, NATO ASI Series, edited by S. P. Beaumont and C. M. Sotomayor Torres (Plenum, New York, 1990), p. 41.

¹¹B. J. van Wees, H. van Houten, C. W. J. Beenakker, J. G. Williamson, L. P. Kouwenhoven, D. van der Marel, and C. T. Foxon, Phys. Rev. Lett. **60**, 848 (1988).

¹²D. A. Wharam, T. J. Thornton, R. Newbury, M. Pepper, H. Ahmed, J. E. F. Frost, D. G. Hasko, D. C. Peacock, D. A. Ritchie, and G. A. C. Jones, J. Phys. C **21**, L209 (1988).

¹³S. Laux and F. Stern, Appl. Phys. Lett. **49**, 91 (1986).

¹⁴U. Meirav, M. A. Kastner, and S. J. Wind, Phys. Rev. Lett. **65**, 771 (1990).